Published in final edited form as:
Mutat Res. 2012 March 1; 731(1-2): 92–98. doi:10.1016/j.mrfmmm.2011.12.004.

Formaldehyde-induced mutagenesis in *Saccharomyces cerevisiae*: molecular properties and the roles of repair and bypass systems

Dennis Grogan[1] and **Sue Jinks-Robertson**
Department of Molecular Genetics and Microbiology, Duke University Medical Center, Durham, N.C. 27710, United States

Abstract

Although DNA-protein cross-links (DPCs) pose a significant threat to genome stability, they remain a poorly understood class of DNA lesions. To define genetic impacts of DPCs on eukaryotic cells in molecular terms, we used a sensitive *Saccharomyces cerevisiae* frameshift-detection assay to analyze mutagenesis by formaldehyde (HCHO), and its response to nucleotide excision repair (NER) and translesion DNA synthesis (TLS). Brief exposure to HCHO was mutagenic for NER-defective *rad14* strains but not for a corresponding *RAD14* strain, nor for a *rad14* strain lacking both Polζ and Polη TLS polymerases. This confirmed that HCHO-generated DNA lesions can trigger error-prone TLS and are substrates for the NER pathway. Sequencing revealed that HCHO-induced single-base-pair insertions occurred primarily at one hotspot; most of these insertions were also complex, changing an additional base-pair nearby. Most of the HCHO-induced mutations required both Polζ and Polη, providing a striking example of cooperativity between these two TLS polymerases during bypass of a DNA lesion formed *in vivo*. The similar molecular properties of HCHO-induced and spontaneous complex +1 insertions detected by this system suggest that DPCs which form *in vivo* during normal metabolism may contribute characteristic events to the spectra of spontaneous mutations in NER-deficient cells.

Keywords

DNA-protein cross-link; frameshift mutations; Complex insertions; DNA Polymerase ζ; DNA Polymerase η

1. INTRODUCTION

DNA-protein or -peptide cross-links (DPCs) are formed *in vivo* by number of chemical agents, such as aldehydes, nickel, chromate and other transition metals, as well as by chemical processes including aerobic respiration, protein oxidation and DNA oxidation [1–4]. The abundance and diversity of endogenous inducers suggest that DPCs are particularly

[1]Permanent address Department of Biological Sciences, University of Cincinnati, 614 Rieveschl Hall, ML0006, Cincinnati OH 45221-0006, United States, 513-556-9748, grogandw@ucmail.uc.edu

CONFLICTS OF INTEREST STATEMENT
The authors declare that they have no conflicts of interest.

frequent and heterogeneous DNA lesions [5–8], and the ability of such adducts to block replication [9] suggests that they pose a significant threat to genome integrity. The molecular diversity of DPCs complicates the development of biochemical assays that are specific to these lesions yet sufficiently sensitive to detect them at biologically relevant levels [1, 10]. Genetic effects offer alternative indicators of DPCs *in vivo*, but many such effects studied historically have been large-scale changes scored microscopically in individual cells ([11, 12]. The genetic burden imposed by DPCs thus remains difficult to assess experimentally at the molecular level.

Of the agents known to induce DPCs *in vivo*, formaldehyde (HCHO) has important advantages for experimental analysis of the impact of DPCs in a well-characterized genetic system . Its ability to cross-link amino compounds to DNA *in vivo* forms the basis of widely used chromatin immunoprecipitation assays, and its mode of action is relatively well-defined and specific ([13–15]. Consistent with these properties, HCHO is carcinogenic and genotoxic at low concentrations, and DPCs appear to be the biologically relevant product of exposure [12, 16–17].

In budding yeast, at least three major pathways cope with HCHO-induced DNA damage: nucleotide excision repair, homologous recombination, and translesion synthesis (NER, HR, and TLS, respectively) [18]. Current models for DPC repair involve an initial proteolysis of covalently attached protein, which reduces it to a relatively small polypeptide; the remaining peptide-DNA adduct can then be excised by NER endoncleases [19, 20]. The importance of this repair pathway in *Saccharomyces cerevisiae* is illustrated by the observation that survival of brief exposure to high HCHO concentrations requires a functioning NER system [21]. NER may also remove the initial DNA adducts of low-molecular weight compounds directly, without requiring prior proteolysis [22]. A second, HR-dependent, pathway also plays an important role in coping with HCHO-induced damage, as indicated by the observation that survival of continuous exposure to low HCHO concentrations seems to depend heavily on proteins required for HR [21]. HR may also be the primary strategy for coping with recalcitrant DPCs that cannot be reduced in size [22, 23].

The third HCHO-coping mechanism, TLS, has received less attention, but, to the degree that it generates a characteristic mutation at, or near, the site of a replication-blocking lesion, TLS has the potential to locate and quantify HCHO-induced DPCs *in vivo* with great sensitivity. Little information is available on molecular aspects of HCHO-associated mutagenesis, however. HCHO is only moderately mutagenic in most genetic assays ([24–27], which is consistent with the possibility that DPCs may be too bulky for TLS or the fact that they can be processed by error-free pathways [28]. The most detailed analyses of HCHO-induced mutagenesis and the relative contributions of accurate vs. error-prone systems have come from specialized bacterial strains that differ significantly in functional and mechanistic terms from eukaryotic cells [6]. For a eukaryotic system, the proportion of HCHO- induced mutagenesis that is due to TLS has not been confirmed, nor have the roles of individual polymerases been investigated. Here, we used a frameshift-reversion assay in *S. cerevisiae* to investigate the ability of HCHO to generate DNA lesions that are normally removed by NER but can be by-passed by TLS polymerases. The results demonstrate that, in the absence of NER, mutagenic bypass of persistent HCHO-generated lesions does occur and that it requires the Polζ TLS polymerase and produces particular types of mutations. There is an additional requirement of the Polη TLS polymerase for some mutation types, providing the first molecular evidence that Polζ and Polη cooperate to bypass DNA damage generated *in vivo*.

2. MATERIAL AND METHODS

2.1. Culture conditions

Unless otherwise indicated, non-selective growth was at 30°C in YPD broth (1% Bacto yeast extract, 2% Bacto Tryptone, 2% D-glucose) with constant aeration by gyrorotary shaking, or on YPD plates containing 1.8% agar. Synthetic dextrose (SD) medium was supplemented with all nutrients except the one selected for prototrophy. Lys^+ revertants were selected on SD-Lys medium, and canavanine-resistant (Can-R) mutants were selected on SD-Arg medium supplemented with L-canavanine sulfate to 60 μg/ml.

2.2. Survival and mutagenesis following HCOH treatment

To measure killing, cultures growing exponentially in YPD medium were harvested, washed twice in sterile distilled water and resuspended in the original volume of sterile distilled water. Half of each washed culture was supplemented with 10 mM HCOH and the other half served as the “no treatment” control. After 30 min at room temperature, cells were washed with water and aliquots of appropriate dilutions were plated on YPD. Colonies were counted after 2 days incubation.

To measure mutagenesis, a set of independent liquid cultures was grown in 0.25 ml of YPD overnight. Cultures were diluted to 1.7 ml in YPD and aerated for an additional 4–5 hours. The cells were pelleted, washed free of residual medium in sterile distilled water, and divided into two equal portions. The treated portion received HCHO (5 mM, unless otherwise noted) and the control portion received only water. After 30 min at room temperature, cells were pelleted and washed free of residual HCHO. Each portion was then resuspended in 0.4 ml YPD and incubated overnight to a final population size of about 1.5×10^8 viable cells. Overnight incubation was determined empirically to yield higher and more reproducible mutant frequencies relative to plating HCHO-treated cells directly onto selective media. In general, one-fifth of the overnight culture was spread on SD-Arg+Can plates to select Can-R mutants, and the remainder was spread on SD-Lys to select Lys^+ revertants. Each experiment was performed on a set of eight independent cultures, and the results of several experiments were combined for the calculation of the median mutant frequency for each strain..

To sample the molecular spectra of Lys^+ reversion events, one revertant colony was retained from each independent culture used in mutation-rate measurements; additional mutants were isolated from independent cultures treated with HCHO and plated for revertants as described above. Genomic DNA was extracted from each clonally purified revertant, and the region including the reversion window of the *lys2ΔA746,NR* allele was amplified by PCR. The resulting products were sequenced, and the mutation in each phenotypic revertant was identified by multiple sequence alignment.

3. RESULTS

3.1. Assay Development

In order to quantify mutagenesis, we first investigated treatment conditions that would mitigate the genotoxic effects of formaldehyde, i.e., produce significant DNA damage but limit the killing of repair-deficient strains. These tests also indicated the relative importance of various TLS polymerases for survival of HCHO challenge. A 30 min exposure of a WT (i.e., repair-proficient) strain to 10 mM HCHO at room temperature was found to yield ~90% survival relative to that of mock-treated cells (Table 1). The NER pathway was inactivated by deleting the *RAD14* gene, and its loss was accompanied by a 5–6 fold reduction in viability following a similar exposure to HCHO. The sensitivity of the *rad14Δ*

strain to HCHO increased about two-fold upon the additional deletion of *REV3*, which encodes the catalytic subunit of Pol ζ, whereas inactivation of Pol η (*rad30Δ*) in the NER-deficient strain had no significant effect on viability (Table 1). Based on these and other results, the treatment scheme we adopted for mutagenesis used a brief exposure to 5 mM HCHO. Each independent culture of a set was split into two aliquots, one of which was HCHO- and the other mock-treated for 30 min. Survival of this HCHO treatment was at least 50% for the *rad14Δ* derivatives and higher for the *RAD14* strain. The resulting cells were then grown for 2–3 generations in the absence of HCHO and plated to enumerate the total numbers of viable and mutant cells for each treated population and its mock-treated duplicate.

Two different assays were used to measure HCHO-associated mutagenesis in WT, *rad14Δ* single, *rad14Δ rev3Δ* and *rad14Δ rad30Δ* double, and *rad14Δ rev3Δ rad30Δ* triple mutant backgrounds. The *CAN1* forward mutation assay detects mutations that inactivate the encoded arginine transporter and result in resistance to the drug canavanine, a toxic arginine analog. The second assay selects net +1 mutations that restore the correct reading frame of the *LYS2* gene (*lys2ΔA746,NR* reporter) [29]. For both assays, the rate of mutant formation was determined following HCHO- vs. mock-treatment of cells (Table 2). Treatment of the WT strain with 5mM HCHO induced negligible mutagenesis in either the forward or reverse assay. There was, however, evidence of HCHO-associated mutagenesis in the *rad14Δ* single and *rad14Δ rad30Δ* double mutants. While the mutagenesis detected by the *CAN1* assay in the *rad14* background was clearly dependent on the presence of Rev3/Polζ, only about half of the *lys2ΔA746,NR* reversion events appeared to require Rev3/Polζ. As will be detailed below, however, sequence analysis revealed distinctive Polζ-dependent changes in the mutation spectrum following the induction of mutagenesis in the *rad14Δ* background. Together, these results indicate that DNA lesions induced by HCHO can be repaired by NER, and that the persistence of lesions can lead to mutation or cell death.

3.2. Molecular properties of frameshift mutations

To examine the molecular nature of HCHO-induced mutations in yeast, we sampled the spectra of +1 frameshift mutations recovered in the *lys2ΔA746,NR* assay in the various NER-defective backgrounds. With this mutational target, any net +1 frameshift event that occurs within a window of ~150 bp restores enzyme activity and can be selected as a phenotypic reversion event [29]. Untreated *rad14Δ* cells, representing the background of mutations that result spontaneously from NER-reparable lesions and other sources, yielded several distinct types of frameshift mutations (Fig. 1A). Approximately 50% (58/114) of the revertants contained 1-bp insertions, and these were fairly equally distributed between two classes: simple events containing only an additional base pair (33/114 = 29%), and complex insertions (“cins”), in which the selected event was accompanied by a nearby base substitution (25/114 = 22%). Such complex events have been previously described in this assay and derive exclusively from Polζ-dependent TLS [30]. The spontaneous complex insertions observed here in the *rad14* mutant were distributed over at least 19 sites within the reversion window. In addition to simple and complex insertions, there were smaller numbers of 4-bp insertions (generally tandem duplications), simple 2-bp deletions, and other minor deletion classes. Finally, either of two large deletions with direct repeats at their ends accounted for ~25% of the mutants sequenced.

The corresponding mutation spectrum from HCHO-treated *rad14Δ* cells had a similar proportion of large deletions (Fig. 1B). Insertions of a single base were more frequent than in the untreated cells, however (96/147 = 65%). This reflected a similar proportional yield of simple 1-bp insertions (44/147 = 30%) as in WT combined with a larger proportion (52/147 = 35%) of complex +1 events. Comparison of the two spectra further revealed that almost half (46/96) of the HCHO-induced, +1 frameshifts occurred at one site in the target (5’-

TTTCAAA; highlighted in yellow). Frameshifts at this site were primarily of three types: simple expansion of the 3A run to 4A (indicated as red "+" in spectra), expansion of 3A to 4A accompanied by a C to T transversion (or 3T > 4T plus C > A; red "cins"), or expansion of 3A to 4A accompanied by a C to A transversion (green "cins"). We designated these three classes type 1, 2 or 3 events, respectively, and their numbers are summarized in Table 3.

The very strong HCHO-induced hotspot observed in the *rad14Δ* strain suggests that HCHO-promoted DNA lesions at this position are normally repaired by NER. To confirm this, we analyzed mutants isolated from the parental NER-proficient strain following treatment with HCHO (Fig. 1C). The resulting spectrum resembled the other two spectra with respect to large repeat-associated deletions, but differed from each of them in other respects. Compared to the HCHO-treated *rad14Δ* mutant, the treated *RAD14* strain had more tandem duplications, and markedly fewer complex single-base insertions (8/137 = 6%). In particular, the strong hotspot that dominated the spectrum of the *rad14Δ* mutant was not represented in the *RAD14* spectrum, confirming that the underlying lesion is normally a substrate for the NER machinery.

The most frequent HCHO-induced mutations in the *rad14Δ* strain were simple and complex 1-bp insertions at the hotspot defined by the sequence 5'-TTTCAAA (Fig. 1B). Abdulovic *et al.* [31] reported previously that this particular region of *lys2ΔA746* (designated "HS3") accumulated large numbers of spontaneous, complex 1-bp insertions in an NER-defective background, and that its activity as a hotspot was affected in opposing directions by the Polζ and Polη TLS polymerases. Specifically, the complex events at HS3 were only evident in the absence of Polη, and were completely dependent on the presence of Polζ [31]. This reciprocal pattern suggested that the underlying spontaneous lesion(s) defining HS3 normally provide a substrate for Polη-dependent bypass, with bypass occurring in a manner that did not yield a detectable mutation (net +1 frameshift). In the absence of Polη, however, Polζ stepped in to accomplish the bypass, but did so in a highly error-prone manner to produce complex mutations.

As noted above, our mutagenesis assays using the *CAN1* forward and *lys2ΔA746,NR* reversion assays indicated that the majority of HCHO-induced mutations require Polζ, but are not affected by the presence/absence of Polη (Table 2). Given the complex interplay of Polζ and Polη with respect to spontaneous lesion bypass (an effect evident only in mutation spectra), we examined the molecular effects of these TLS polymerases on HCHO-induced mutations in the *rad14Δ* mutant. The corresponding spectra of Lys^+ revertants confirmed that the complex mutations at HS3 required Polζ, as did most of the complex events elsewhere in this reversion window (Figs. 1B and 2A). In addition, the simple +1 mutations at HS3 were dependent on Polζ; 19/147 mutations were of this type in the *rad14Δ* single mutant, compared to 0/112 mutations in the *rad14Δ rev3Δ* double mutant (Fig. 2A). In striking contrast to the increase in spontaneous HS3 events observed previously upon Polη loss [31], two of the three classes of HCHO-induced mutations at HS3 (types 1 and 2) were significantly reduced in the *rad14Δ rad30Δ* double relative to the *rad14Δ* single mutant; type 3 events were not affected by Polη loss (Fig. 2B and Table 3). As in the *rad14Δ rev3Δ* background, however, HS3 was not seen in the *rad14Δ rad30Δ rev3*Δ background (Fig. 2C). These data suggest that bypass of some HCHO-induced lesions at HS3 jointly requires Polη and Polζ, while other bypass requires only Polζ. Finally, it should be noted that several complex insertions were evident in the HCHO-induced spectrum of the *rad14Δ rev3Δ* strain (7/112 = 6%), but there were none (0/100) in the *rad14Δ rad30Δ rev3Δ* spectrum (P = 0.01). There may thus be some rare types of complex events that are independent of Polζ, but require Polη.

4. DISCUSSION

4.1. Genetic consequences of formaldehyde treatment

This study presents a molecular-genetic analysis of formaldehyde-induced mutations in a model eukaryote and provides new insight into how cells cope with bulky, replication-blocking DNA-protein and -peptide crosslinks (DPCs). Consistent with results from other studies, treatment of NER-proficient cells with an HCHO dose that caused little, if any, killing did not increase overall mutant frequencies [12]. Treatment of NER-deficient strains with the same HCHO dose, however, reduced viability ~80% and enhanced mutagenesis 2–4 fold among survivors. HCHO-induced mutagenesis was evident both in the *CAN1* forward mutation assay and in the *lys2ΔA746,NR* frameshift reversion assay. The relative increase was somewhat higher for *lys2* frameshift reversion than for *CAN1* inactivation, but the latter target is expected to provide a much greater diversity of HCHO-induced mutations. Nevertheless, our observations indicate that, under the conditions tested, HCHO generates potentially lethal and mutagenic DNA lesions in both target genes, many of which are usually repaired by the NER pathway before the affected DNA is replicated. These biological responses are consistent with the biochemical evidence that many HCHO-induced DNA lesions are bulky adducts formed by cross-linking a protein, peptide, or other endogenous amine to DNA [14, 15].

The effect of HCHO treatment on overall mutant frequencies in NER-defective strains was modest, but analyses of the corresponding *lys2ΔA746,NR* reversion spectra revealed that not all classes of mutations were equally affected. This is evident in Table 4, which presents the rates of individual types of HCHO- induced mutations in the different genetic backgrounds analyzed. The rate of large deletions bordered by direct repeats, for example, was elevated 2-fold following HCHO treatment of the *rad14* strain. Previous work has argued that such deletions reflect the repositioning of a 3’ end when DNA replication is blocked by a lesion [31], and their increase in response to brief HCHO treatment is consistent with formation of replication-blocking DPCs. Although the proportions of large deletions increased upon additional loss of Polζ (in *rev3* mutants), the rates of these deletions did not increase. This suggests that the HCHO-induced lesions which promote large deletions may not provide favorable substrates for direct bypass, perhaps because they are too bulky to be accommodated in the active site pocket of the enzyme.

4.2. Complex single-basepair insertions

Previous studies of *lys2ΔA746,NR* reversion demonstrated that complex insertions (“cins”), defined as frameshifts with an associated base substitution, are a unique signature of Polζ ([29, 30, 31, 33]. Spontaneous cins are elevated in repair-defective backgrounds, suggesting that they reflect the Polζ-dependent bypass of polymerase-blocking lesions that arise during normal metabolism and growth but are usually repaired before replication. The most dramatic alteration in the spectrum of a *rad14* strain in response to HCHO-treatment was the appearance of a strong cins hotspot at the sequence 5’-TTTCAAA (highlighted yellow in Figure 1). Although Abdulovic et al. [31] observed spontaneous Rev3-dependent cins at this position (“HS3”) in an NER-defective background, these spontaneous cins at HS3 were only seen upon loss of Polη. In contrast, the HCHO-induced events at H3 that we observed in the present study were proportionally reduced in a *rad14 rad30* background, suggesting that bypass of DPCs at this position is partially dependent on Polη. A second unusual feature of HCHO-induced frameshifts at HS3, which was not seen previously in spontaneous spectra, was a strong elevation in simple events at this position as well. All simple frameshifts expanded the 3A run to a 4A run (5’-TTTCAAA changed to 5’-TTTCAAAA; see Table 3); we designate these events type 1 mutations and they are indicated in red in Figures 1 and 2. Similar to the HCHO-induced cins at HS3, type 1 events were partially dependent on Polη

and were completely dependent on Polζ (see Figure 2 and Table 3). When the simple and complex events are considered together, we estimate that there was at least a 50-fold increase in the rate of mutations at H3 following the exposure of *rad14* cells to HCHO.

There were two distinct types of HCHO-induced cins that accumulated at HS3 in the *rad14* background (Table 3). In type 2 mutations (indicated in red in Figures 1 and 2), the HS3 sequence changed from 5'-TTTCAAA to 5'-TTTTAAAA, which could reflect either a C > T base substitution accompanied by expansion of the 3A run to a 4A run, or coupled C > A plus 3T > 4T changes. Type 2 events could reflect expansion of either the 3A or 3T run at H3, but type 3 events (5'-TTTCAAA changed to 5'-TTTAAAAA; indicated in green in Figures 1 and 2) can only be explained by a C > A base substitution associated with slippage in the 3A run. Whereas type 3 events were insensitive to the status of Polη, there was a significant reduction in type 2 events in the *rad14 rad30* background. The potential cooperation of Polζ and Polη in lesion bypass has been inferred from *in vitro* studies [34], and the data from the present study demonstrate a co-requirement for these TLS polymerases in bypassing a proportion of HCHOinduced lesions in yeast. Based on *in vitro* studies, we assume that Polη inserts a dNMP opposite the relevant HCHO-generated lesion and that Polζ extends the resulting unpaired terminus.

Previous studies have provided evidence that the base substitution and frameshift of cins are coupled events, with the base substitution marking the position of the initiating lesion and facilitating the subsequent slippage event that produces the selected frameshift [33, 35]. Fig. 3 presents a model for how the three types of HCHO-induced mutations at HS3 could be derived from HCHO-induced DPC(s) at a common position. As noted previously, the 3A run is expanded to 4A in the type 1 and 3 mutations and for simplicity, we will assume that it is also the 3A run (rather than the 3T run) that is expanded in type 2 events. Because our model of cins production proposes that the base substitution is at the position of the initiating lesion and occurs before the slippage event, the initiating lesion (at the CG base pair between the 3N runs) is predicted to be on the 3' side of the run where subsequent slippage occurs. The relevant HCHO-induced DPC must, therefore, reside at the G residue on the noncoding strand; on the coding strand, the complementary C would be encountered after slippage and hence is on the wrong (5') side of the 3A run. *RAD30* is required only for type 1 or 2 events, suggesting that Polη catalyzes insertion of dCMP or dTMP, respectively, opposite the damaged G. The insertion of dAMP to generate type 3 mutations does not require Polη, and could be catalyzed by either Polζ or a replicative DNA polymerase. Because all three types of events require *REV3*, however, we suggest that Polζ is required to extend the termini opposite the initiating DPC. Although the model in Figure 3 can place the initiating lesion for all three types of HS3 events at the same position (the guanine of the CG base pair where base substitutions occur), the three mutagenic outcomes do not appear to be interchangeable; that is, the reduction in type 1 and 2 events in the *rad30* background was not accompanied by compensating increase in the Polη-independent type 3 events. This suggests that the lesion which initiates type 1 and 2 events differs from the lesion that initiates type 3 events with respect to chemical structure or nucleotide position.

4.3. Implications for spontaneous DPCs

The HCHO-induced events reported here resemble in multiple respects certain spontaneous cins observed previously in the *lys2*ΔA746 reversion window, raising the possibility that the spontaneous cins may derive from endogenous DPCs. The spontaneous cins cluster at two hotspots (designated HS1 and HS2) only when nucleotide excision repair (NER) is inactivated and Rev3/Polζ remains functional [29–31]. Both HS1 and HS2 have G residues immediately 3' of a 3T run; the spontaneous cins all expand the 3T run to 4T, and most replace the G with T [31]. The molecular nature of the spontaneous cins at HS1 and HS2 indicates that they, like the HCHO-induced cins at HS3, result from misincorporation

opposite a damaged G residue, followed by expansion (via slippage) of the subsequent mononucleotide tract. Interestingly, these cins also exhibit a physiological requirement, namely aerobic respiration [36]. This property suggests that the damaged G which triggers these mutations is formed by an oxidative process, yet the lesion does not appear to be 7,8-dihydro-8-oxo guanine (8-oxoG), since deletion of *OGG1* had negligible effect on spontaneous cins at HS1 and HS2 [36]. We note, however, that reactive oxygen species are also known to initiate cross-linking of DNA to protein or, conversely, protein to DNA, at G residues [1], so the respiration-dependence of these spontaneous cins and their avoidance by NER would be consistent with initiation by a DPC. Similarly, chromatin structure or other factors are likely to affect the proximity and reactivity of the DNA and protein partners, and may discourage spontaneous DPC formation at similar sequence motifs in the *lys2*ΔA746 reversion window outside of HS1 and HS2 [30].

4.4. Conclusions

Our results indicate that HCHO-treatment of NER-deficient yeast cells provides an experimental system for detailed analysis of genetic impacts of DPCs. The observed killing and mutagenic effects of HCHO, and the responses of these effects to mutations in NER and TLS genes, all corresponded to those predicted for DPCs. HCHO induced a variety of mutations in a frameshift-specific reporter gene, but the mutations attributed to DPCs are predominantly single-nucleotide insertions generated at a specific site *via* co-operation of Polζ and Polη. Nevertheless, a significant minority of the hotspot cins do not require Polη whereas Polη acting alone generates a few cins elsewhere in the frameshift reporter. Most of the molecular properties of the putative DPC-induced frameshifts are shared by spontaneous mutations in the same target gene, implicating these spontaneous mutations as possible products of endogenous DPCs. The basis of the observed sequence-specificity of HCHO-induced frameshifts, and the diversity of non-frameshift mutations that are presumed to be induced by HCHO, represent questions of future interest leading to a fuller elucidation of molecular mechanisms of DPC-induced mutagenesis in eukaryotic cells and the implications for genome stability.

Highlights

- A selection analyzed formaldehyde-induced frameshifts in yeast
- The pre-mutagenic DNA lesions are subject to repair by NER
- Formaldehyde-induced frameshifts cluster at a specific site (TTTCAAA)
- Most of these mutations require both DNA Polζ and DNA Polη

Acknowledgments

We thank K. Lehner for some of the WT data of Table 4, and K. Lehner, N. Kim, and other members of the Jinks-Robertson lab for helpful discussions. This work was supported by grants from NIH to DG (F33 GM088933) and SJR (R01 GM064796).

REFERENCES

1. Barker S, Weinfeld M, Murray D. DNA-protein crosslinks: their induction, repair, and biological consequences. Mutat. Res. 2005; 589:111–135. [PubMed: 15795165]
2. Davies MJ. The oxidative environment and protein damage. Biochim.Biophys.Acta. 2005; 1703:93–109. [PubMed: 15680218]
3. Neeley WL, Essigmann JM. Mechanisms of formation, genotoxicity, and mutation of guanine oxidation products. Chem. Res. Toxicol. 2006; 19:491–505. [PubMed: 16608160]

4. Xie J, Fan R, Meng Z. Protein oxidation and DNA-protein crosslink induced by sulfur dioxide in lungs, livers, and hearts from mice. Inhal. Toxicol. 2007; 19:759–765. [PubMed: 17613084]
5. Voitkun V, Zhitkovich A. Analysis of DNA-protein crosslinking activity of malondialdehyde in vitro. Mutat. Res. 1999; 424:97–106. [PubMed: 10064853]
6. Marnett LJ, Hurd HK, Hollstein MC, Levin DE, Esterbauer H, Ames BN. Naturally occurring carbonyl compounds are mutagens in *Salmonella* tester strain TA104. Mutat. Res. 1985; 148:25–34. [PubMed: 3881660]
7. Cadet J, Berger M, Douki T, Ravanat JL. Oxidative damage to DNA: formation, measurement, and biological significance. Rev. Physiol. Biochem. Pharmacol. 1997; 131:1–87. [PubMed: 9204689]
8. Minko IG, Kozekov ID, Kozekova A, Harris TM, Rizzo CJ, Lloyd RS. Mutagenic potential of DNA-peptide crosslinks mediated by acrolein-derived DNA adducts. Mutat. Res. 2008; 637:161–172. [PubMed: 17868748]
9. Kuo HK, Griffith JD, Kreuzer KN. 5-Azacytidine induced methyltransferase-DNA adducts block DNA replication in vivo. Cancer Res. 2007; 67:8248–8254. [PubMed: 17804739]
10. Zhitkovich A, Costa M. A simple, sensitive assay to detect DNA-protein crosslinks in intact cells and in vivo. Carcinogenesis. 1992; 13:1485–1489. [PubMed: 1499101]
11. Natarajan AT, Darroudi F, Bussman CJ, van Kesteren-van Leeuwen AC. Evaluation of the mutagenicity of formaldehyde in mammalian cytogenetic assays in vivo and vitro. Mutat. Res. 1983; 122:355–360. [PubMed: 6656818]
12. Merk O, Speit G. Significance of formaldehyde-induced DNA-protein crosslinks for mutagenesis. Environ. Mol. Mutagen. 1998; 32:260–268. [PubMed: 9814441]
13. Solomon MJ, Varshavsky A. Formaldehyde-mediated DNA-protein crosslinking: a probe for *in vivo* chromatin structures. Proc. Natl. Acad. Sci. U.S.A. 1985; 82:6470–6474. [PubMed: 2995966]
14. Lorenti Garcia C, Mechilli M, Proietti De Santis L, Schinoppi A, Kobos K, Palitti F. Relationship between DNA lesions, DNA repair and chromosomal damage induced by acetaldehyde. Mutat. Res. 2009; 662:3–9. [PubMed: 19084543]
15. Kuykendall JR, Bogdanffy MS. Efficiency of DNA-histone crosslinking induced by saturated and unsaturated aldehydes *in vitro*. Mutat. Res. 1992; 283:131–136. [PubMed: 1381490]
16. Kerns WD, Pavkov KL, Donofrio DJ, Gralla EJ, Swenberg JA. Carcinogenicity of formaldehyde in rats and mice after long-term inhalation exposure. Cancer Res. 1983; 43:4382–4392. [PubMed: 6871871]
17. Recio L, Sisk S, Pluta L, Bermudez E, Gross EA, Chen Z, et al. P53 Mutations in Formaldehyde-Induced Nasal Squamous Cell Carcinomas in Rats. Cancer Res. 1992; 52:6113–6116. [PubMed: 1394239]
18. Ide H, Nakano T, Salem AM, Terato H, Pack SP, Makino K. Repair of DNA-protein crosslink damage: coordinated actions of nucleotide excision repair and homologous recombination. Nucleic Acids Symp.Ser. (Oxf). 2008; 52:57–58.
19. Minko IG, Zou Y, Lloyd RS. Incision of DNA-protein crosslinks by UvrABC nuclease suggests a potential repair pathway involving nucleotide excision repair. Proc. Natl. Acad. Sci. U.S.A. 2002; 99:1905–1909. [PubMed: 11842222]
20. Quievryn G, Zhitkovich A. Loss of DNA-protein crosslinks from formaldehyde-exposed cells occurs through spontaneous hydrolysis and an active repair process linked to proteosome function. Carcinogenesis. 2000; 21:1573–1580. [PubMed: 10910961]
21. de Graaf B, Clore A, McCullough AK. Cellular pathways for DNA repair and damage tolerance of formaldehyde-induced DNA-protein crosslinks. DNA Repair (Amst). 2009; 8:1207–1214. [PubMed: 19625222]
22. Nakano T, Morishita S, Terato H, Pack SP, Makino K, Ide H. Repair mechanism of DNA-protein cross-link damage in Escherichia coli. Nucleic Acids Symp. Ser. (Oxf). 2007; 51:213–214.
23. Reardon JT, Sancar A. Repair of DNA-polypeptide crosslinks by human excision nuclease. Proc. Natl. Acad. Sci. U.S.A. 2006; 103:4056–4061. [PubMed: 16537484]
24. Goldmacher VS, Thilly WG. Formaldehyde is mutagenic for cultured human cells. Mutat. Res. 1983; 116:417–422. [PubMed: 6835255]
25. Craft TR, Bermudez E, Skopek TR. Formaldehyde mutagenesis and formation of DNA-protein crosslinks in human lymphoblasts in vitro. Mutat. Res. 1987; 176:147–155. [PubMed: 3796657]

26. Takahashi K, Morita T, Kawazoe Y. Mutagenic characteristics of formaldehyde on bacterial systems. Mutat. Res. 1985; 156:153–161. [PubMed: 3889633]
27. Zijlstra JA. Liquid holding increases mutation induction by formaldehyde and some other cross-linking agents in Escherichia coli K12. Mutat. Res. 1989; 210:255–261. [PubMed: 2643024]
28. Yamanaka K, Minko IG, Finkel SE, Goodman MF, Lloyd RS. The role of high fidelity E. coli DNA polymerase I in the replication bypass of deoxyadenosine DNA-peptide cross-link. J. Bacteriol. 2011
29. Lehner K, Jinks-Robertson S. The mismatch repair system promotes DNA polymerase zeta-dependent translesion synthesis in yeast. Proc. Natl. Acad. Sci. U.S.A. 2009; 106:5749–5754. [PubMed: 19307574]
30. Minesinger BK, Jinks-Robertson S. Roles of RAD6 epistasis group members in spontaneous polzeta-dependent translesion synthesis in *Saccharomyces cerevisiae*. Genetics. 2005; 169:1939–1955. [PubMed: 15687278]
31. Abdulovic AL, Minesinger BK, Jinks-Robertson S. Identification of a strand-related bias in the PCNA-mediated bypass of spontaneous lesions by yeast Pol(eta). DNA Repair (Amst). 2007; 6:1307–1318. [PubMed: 17442629]
32. Kim N, Abdulovic AL, Gealy R, Lippert MJ, Jinks-Robertson S. Transcription-associated mutagenesis in yeast is directly proportional to the level of gene expression and influenced by the direction of DNA replication. DNA Repair (Amst). 2007; 6:1285–1296. [PubMed: 17398168]
33. Harfe BD, Jinks-Robertson S. DNA polymerase zeta introduces multiple mutations when bypassing spontaneous DNA damage in *Saccharomyces cerevisiae*. Mol. Cell. 2000; 6:1491–1499. [PubMed: 11163221]
34. Haracska L, Unk I, Johnson RE, Johansson E, Burgers PM, Prakash S, et al. Roles of yeast DNA polymerases delta and zeta and of Rev1 in the bypass of abasic sites. Genes Dev. 2001; 15:945–954. [PubMed: 11316789]
35. Kim N, Jinks-Robertson S. dUTP incorporation into genomic DNA is linked to transcription in yeast. Nature. 2009; 459:1150–1153. [PubMed: 19448611]
36. Minesinger BK, Abdulovic AL, Ou TM, Jinks-Robertson S. The effect of oxidative metabolism on spontaneous Pol zeta-dependent translesion synthesis in *Saccharomyces cerevisiae*. DNA Repair (Amst). 2006; 5:226–234. [PubMed: 16290107]

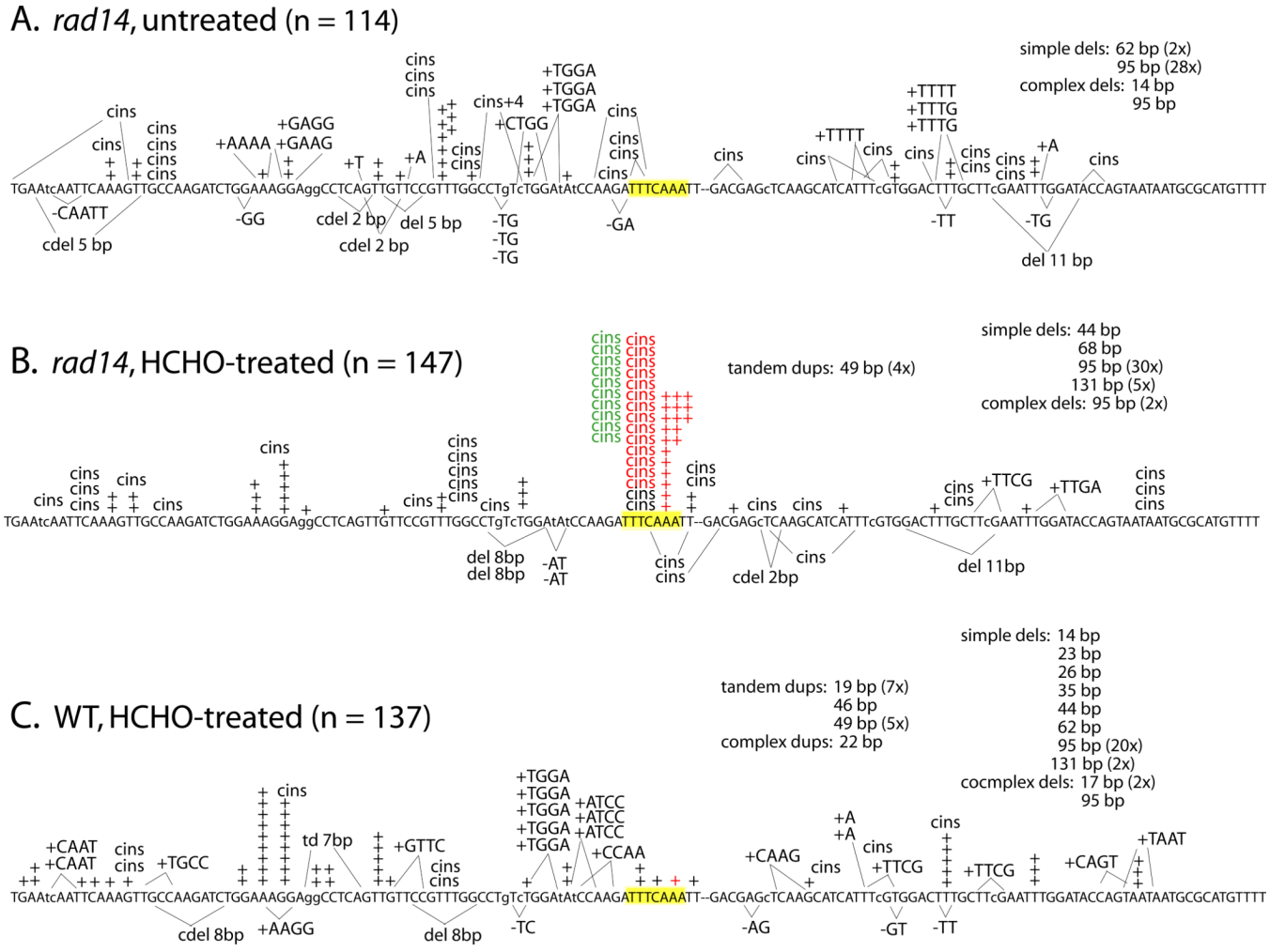

Figure 1.

Effect of formaldehyde treatment and NER status on frameshift mutagenesis. The nucleotide sequence represents the reversion window of the *lys2ΔA746,NR* allele, in which the position of the deleted A is marked by a hyphen. Each event affecting fewer than 12 bp is represented individually; larger events are summarized under captions. Small insertions and deletions are indicated above and below the sequence, respectively; complex insertions are designated “cins”. HS3 is highlighted yellow; type 1 and 2 events are in red and type 3 events are in green.

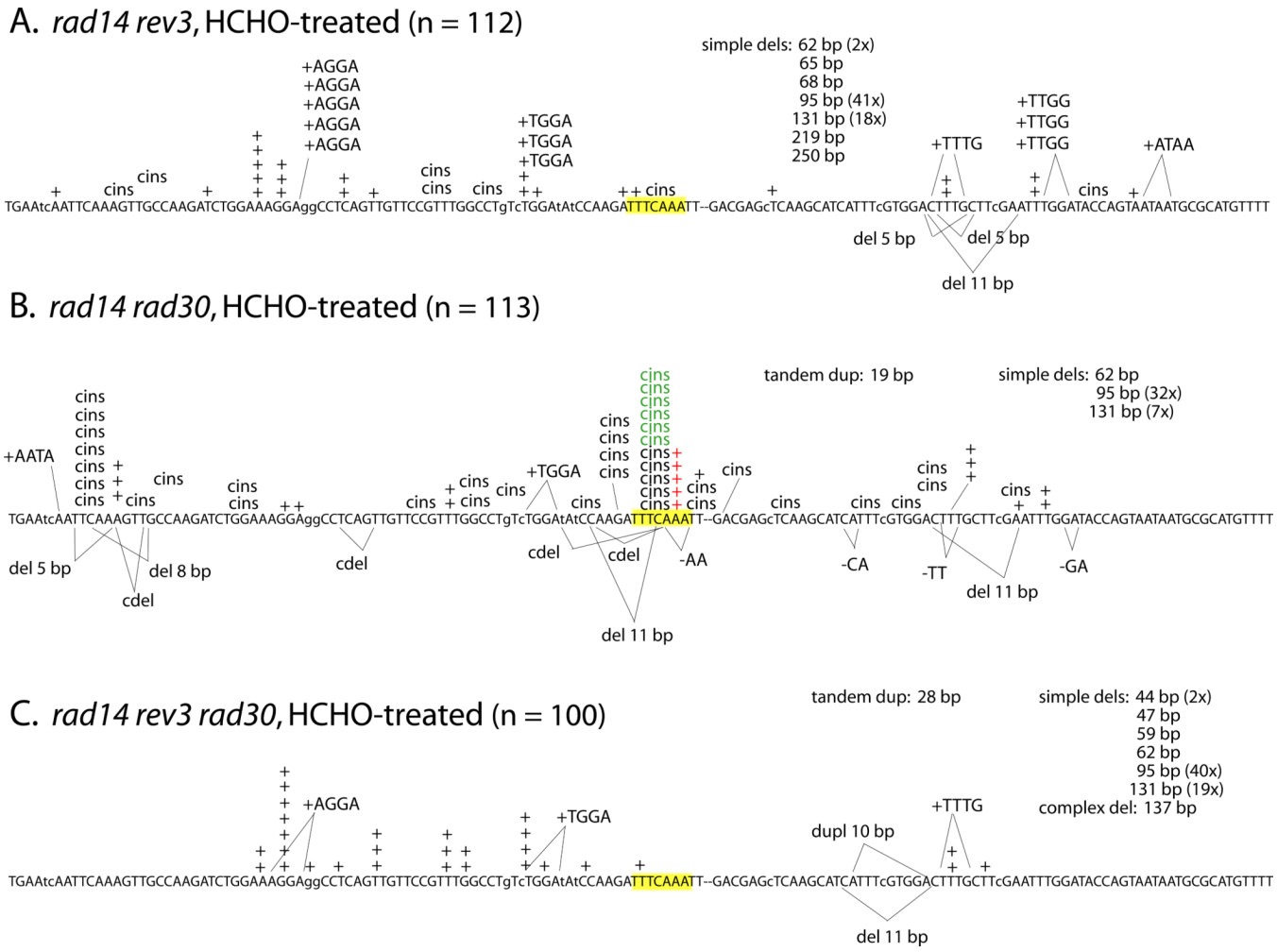

Figure 2.
Effect of TLS polymerases on formaldehyde-induced frameshift mutagenesis. See Figure 1 legend for details.

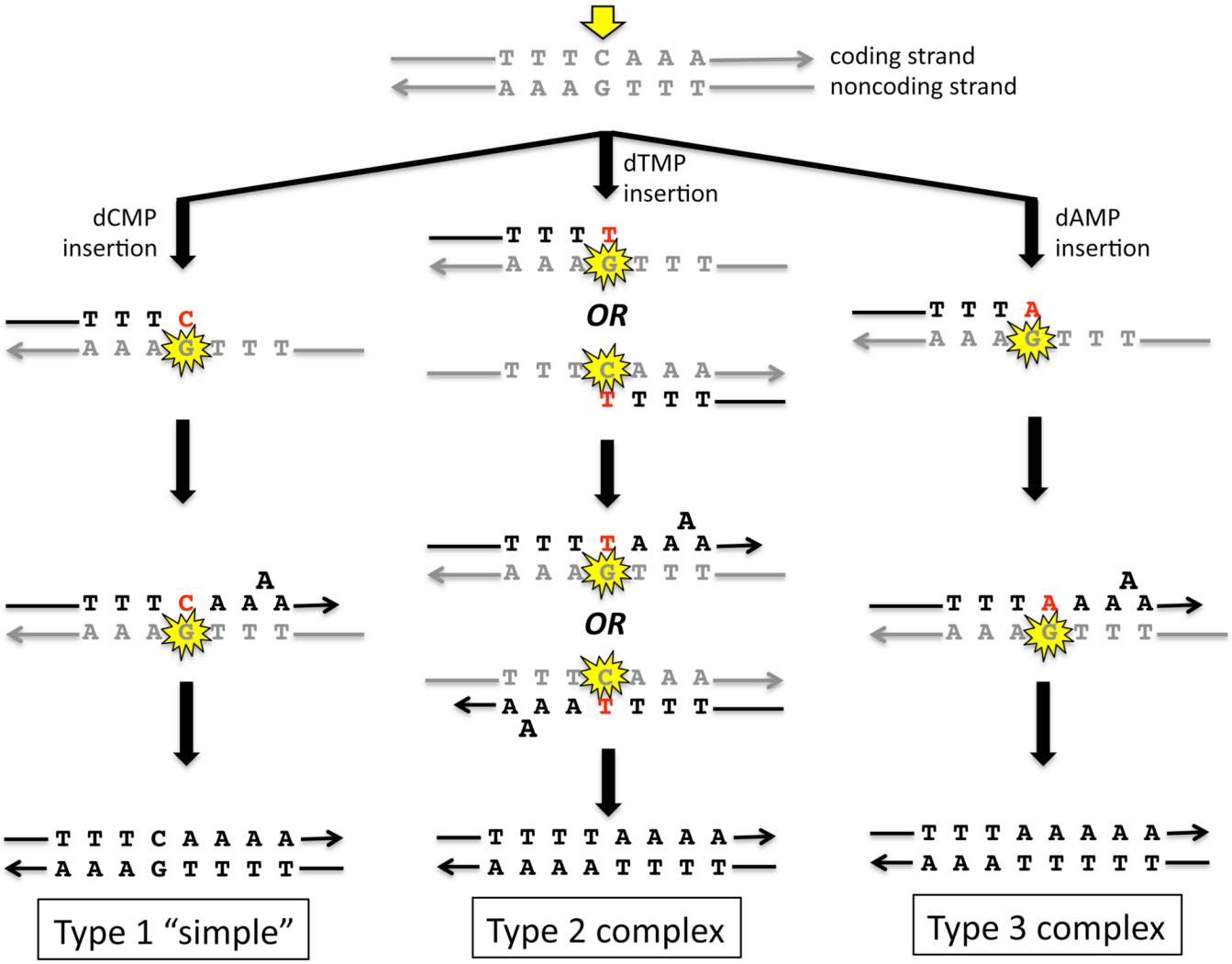

Figure 3.

Proposed mechanisms for formaldehyde-induced mutagenesis at the hotspot "HS3". The three schemes summarize events catalyzed by Polζ and Polη that can generate the observed HCHO-induced, Rev3-dependent complex insertions. For simplicity the initiating DPC (indicated by the yellow star) is depicted at the guanine between the 3T and 3A runs, but other positions are possible. The base inserted opposite the initiating DPC is in red.

Table 1

Roles of NER and TLS in survival of formaldehyde treatment[a]

Strain	Genotype	Mean (± SD)	Relative to WT
SJR1467	WT	0.870 ± 0.155	1.0
SJR2645	*rad14*	0.155 ±0.064	0.18
SJR2671	*rad14 rev3*	0.084 ± 0.043[b]	0.10
SJR3138	*rad14 rad30*	0.204 ± 0.127[b]	0.24
SJR3139	*rad14 rev3 rad30*	0.109 ± 0.068	0.13

[a]Cells were treated with 10 mM formaldehyde for 30 min at room temperature and plated immediately. Viability was measured relative to mock-treated cells from the same culture; data are based on three independent experiments.

[b]P = 0.119 by one-tailed T test.

Table 2

Roles of NER and TLS in formaldehyde mutagenesis

NER, TLS Genotype	n[a]	Forward Mutation (*CAN1*) Median Mutant Frequency, 10^{-6} control (sham)	(95% CI)	HCHO-treated	(95% CI)	-fold change[b]	Frameshift Reversion (*lys2*ΔA746) Median Mutant Frequency, 10^{-8} control (sham)	(95% CI)	HCHO-treated	(95% CI)	-fold change[b]
wild-type	24	1.73	(1.09 –2.18)	1.69	(1.01 – 2.09)	1.0	0.43	(0 – 0.63)	0.32	(0 – 0.80)	0.7
rad14	23	2.95	(1.85 – 4.56)	6.24	(5.06 – 8.40)	2.1	0.60	(0 – 2.31)	2.00	(0.89 – 3.31)	3.3
rad14 rev3	16	0.48	(0.26 – 1.07)	0.57	(0.33 – 1.32)	1.2	0.43	(0 – 1.68)	0.82	(0 – 1.37)	1.9
rad14 rad30	24	2.61	(1.90 – 3.29)	5.58	(4.43 – 6.76)	2.1	0.78	(0 – 1.50)	1.59	(0.77 – 4.36)	2.1
rad14 rad30 rev3	24	0.72	(0.56 – 1.27)	0.74	(0.45 – 1.12)	1.0	0.49	(0 – 0.96)	0.52	(0 – 1.60)	1.0

[a] Number of independent cultures split into two and subjected to sham *vs.* formaldehyde treatment

[b] Ratio of treated:control mutant frequencies

Table 3

Types and number of HCHO-induced events at the TTTCAAA hotpsot

	New sequence at hotspot	Number of events observed[a]			
Type	**[mutations]**	**WT**	***rad14***	***rad14 rad30***	***rad14 rev3***
1	TTTC*AAAA*	1	19	5	0
	[3A > 4A]			(P=0.014)	(P<0.001)
2	TTTTAAAA	0	14	0	0
	[C > T, 3A > 4A or C > A, 3T >4T]			(P<0.001)	(P<0.001)
3	TTT*A**AAAA*	0	10	6	0
	[C > A and 3A > 4A]			(P=0.41)	(P=0.003)
	Other complex	0	2	5	1
	Total mutants sequenced	137	147	113	112

[a]P values were obtained using the Fisher Exact test to compare the numbers of a given event in the *rad14* single and indicated double mutants.

Table 4

Induction of specific mutation types in WT and NER-defective strains

Genotype	Lys$^+$ rate (× 10^{-9})[a]					
	+1	**cins**	**dups ≥ 4 bp**	**2-bp del**	**dels ≥ 5 bp**	**Total**
WT untreated[b]	1.2 (64/169)	0.20 (11/169)	0.34 (19/169)	0.42 (23/169)	0.95 (52/169)	3.1
WT + HCHO	1.3 (58/137)	0.18 (8/137)	0.77 (34/137)	0.09 (4/137)	0.75 (33/137)	3.1
rad14 untreated	1.4 (33/114)	1.1 (25/114)	0.47 (11/114)	0.40 (9/114)	1.5 (36/114)	4.9
Rad14 + HCHO	3.1 (44/147)	3.6 (52/147)	0.42 (6/147)	0.21 (3/147)	2.9 (42/147)	10.2
Rad14 rev3 + HCHO	1.2 (24/112)	0.36 (7/112)	0.66 (13/112)	0.05 (0/112)	3.5 (68/112)	5.7
Rad14 rad30 + HCHO	1.6 (18/113)	3.6 (40/113)	0.27 (3/113)	0.73 (8/113)	4.0 (44/113)	10.3
Rad14 rev3 rad30 + HCHO	1.4 (29/100)	0.05 (0/100)	0.29 (6/100)	0.10 (2/100)	3.2 (65/100)	4.9

[a] Dups, duplications; del(s), deletions(s); cins, complex insertions

[b] Data of K. Lehner (unpublished).